

## Retraction

# Retracted: The Influence of Multisensor Fusion Machine Learning on the Controllable Fabrication of MOF (UIO-66)/ZrAl Ceramic Composite Membranes

### Journal of Sensors

Received 23 January 2024; Accepted 23 January 2024; Published 24 January 2024

Copyright © 2024 Journal of Sensors. This is an open access article distributed under the Creative Commons Attribution License, which permits unrestricted use, distribution, and reproduction in any medium, provided the original work is properly cited.

This article has been retracted by Hindawi following an investigation undertaken by the publisher [1]. This investigation has uncovered evidence of one or more of the following indicators of systematic manipulation of the publication process:

- (1) Discrepancies in scope
- (2) Discrepancies in the description of the research reported
- (3) Discrepancies between the availability of data and the research described
- (4) Inappropriate citations
- (5) Incoherent, meaningless and/or irrelevant content included in the article
- (6) Manipulated or compromised peer review

The presence of these indicators undermines our confidence in the integrity of the article's content and we cannot, therefore, vouch for its reliability. Please note that this notice is intended solely to alert readers that the content of this article is unreliable. We have not investigated whether authors were aware of or involved in the systematic manipulation of the publication process.

Wiley and Hindawi regrets that the usual quality checks did not identify these issues before publication and have since put additional measures in place to safeguard research integrity.

We wish to credit our own Research Integrity and Research Publishing teams and anonymous and named external researchers and research integrity experts for contributing to this investigation.

The corresponding author, as the representative of all authors, has been given the opportunity to register their agreement or disagreement to this retraction. We have kept a record of any response received.

### References

- [1] X. Xu, X. Yang, S. Shao, C. Zhu, and X. Xu, "The Influence of Multisensor Fusion Machine Learning on the Controllable Fabrication of MOF (UIO-66)/ZrAl Ceramic Composite Membranes," *Journal of Sensors*, vol. 2022, Article ID 3039064, 9 pages, 2022.

## Research Article

# The Influence of Multisensor Fusion Machine Learning on the Controllable Fabrication of MOF (UIO-66)/ZrAl Ceramic Composite Membranes

Xiaobing Xu <sup>1,2</sup>, Xu Yang,<sup>1</sup> Shiyuan Shao,<sup>1</sup> Chunling Zhu,<sup>1</sup> and Xiaoyong Xu <sup>1,2</sup>

<sup>1</sup>College of Material Science and Engineering, Chaohu University, Hefei 238000, China

<sup>2</sup>Key Laboratory of Functional Material Processing and Application, Chaohu University, Hefei 238000, China

Correspondence should be addressed to Xiaoyong Xu; 053063@chu.edu.cn

Received 22 April 2022; Revised 15 June 2022; Accepted 22 June 2022; Published 27 July 2022

Academic Editor: Yuan Li

Copyright © 2022 Xiaobing Xu et al. This is an open access article distributed under the Creative Commons Attribution License, which permits unrestricted use, distribution, and reproduction in any medium, provided the original work is properly cited.

This study is aimed at improving the utilization efficiency of resources and enhancing the experiments' effect of various composite membrane research. Firstly, the meaning and preparation process of Metal-Organic Frameworks (MOFs) are discussed. Then, the theoretical knowledge of fusing machine learning and multisensor technology is outlined. Finally, based on the controllable fabrication concept of MOF [UIO- (Universitetet I Oslo-) 66]/ZrAl ceramic composite membranes, a multisensor model incorporating machine learning is designed. The results show that the designed radial sensor backpropagation (RS-BP) fusion multisensor model has the highest error rate of about 0.87. When the number of training is about 100 times, the model's error rate tends to be stable, and the minimum error rate is about 0.01. Secondly, the maximum adsorption capacity of the composite membrane under the controllable preparation of the model is 800 cm<sup>3</sup>/g Spanning Tree Protocol (STP). Additionally, the adsorption capacity decreases slowly, and the overall adsorption energy is higher than that of the traditional preparation method. Finally, the catalytic efficiency of membranes prepared by fusing multiple sensors is 90%-97%. The research achieves innovation in technology and improves the feasibility of rational application of MOF (UIO-66)/ZrAl ceramic composite membranes. This study not only provides technical support for the development of machine learning fusion multisensing technology but also contributes to the comprehensive improvement of the resource utilization effect.

## 1. Introduction

With the development of science and technology, a variety of sensor technologies are widely used in human society, providing a lot of technical support for the development of human society. Additionally, it has developed tremendously on its own and merged with a variety of other technologies to create more technical approaches. As a relatively advanced and widely used science and technology, machine learning and sensor fusion play an important role in the innovation and expansion of the two [1]. MOF (UIO-66) [Metal-Organic Frameworks (Universitetet I Oslo-66)]/ZrAl ceramic composite membrane provides great technical support in human research experiments and social and environmental governance. It is necessary to optimize it by scientific

and technological means to improve its comprehensive performance [2].

Zhang et al. pointed out that Metal-Organic Framework (MOF) compounds known as coordination polymers were developed about 20 years ago. MOF compounds have infinite lattices, which are mainly composed of two main components (metal ions or clusters), inorganic lattice, and organic network structure. The two main components are linked to each other by coordination bonds and also react with other indirect molecules to form an infinite topology with pore structures occupied by solvent molecules. In recent years, MOFs have attracted extensive attention as a relatively new porous material in the literature reports in the field of MOFs. In recent decades, the development of multifunctional applications of MOFs has attracted more

scientists' interest than more excellent new structures and explorations in earlier decades. Since the structure of MOFs is closely related to their potential properties, the design of their structure and the exploration of their properties have become very important topics. Most of the structural properties of MOFs are occupied by their pores. Therefore, the construction of MOFs with suitable pore size, shape, and environment is very attractive and more helpful for their functional applications [3]. Li et al. pointed out that traditional energy consumption has accelerated, and the problem of climate change has become increasingly prominent. Therefore, nuclear energy has become an important choice for energy development in various countries and regions. However, nuclear safety and environmental issues are the bottlenecks restricting the development of nuclear power, especially the removal and enrichment of uranium from radioactive wastewater and the extraction of uranium from seawater which are closely related. Therefore, searching for efficient, fast, and selective uranium separation nanoporous materials is of great significance. MOFs are a new member of the nanoporous material family, which have attracted more and more attention and research due to their porosity, large specific surface area, and structural diversity [4]. Shepelev et al. pointed out that the neural network can self-organize and self-learn and adaptively discover the inherent characteristics and regularities contained in the sample data during the learning process. This self-learning capability is different from the methods employed in traditional pattern recognition. The latter often relies on the programmer's prior knowledge of the recognition rules. Additionally, the neural network does not need to make any assumptions about the distribution state of the object to be processed in the sample space but directly learns the relationship between samples from the data. Thus, they can also solve recognition problems that cannot be solved because the sample distribution is unknown [5]. At present, metal frameworks have been widely used in social industries, but the research on their preparation technology is not perfect. In the process of its application, the influence of uncontrollable factors is very large, and more research is needed to provide technical support for its controllable preparation and improve the rational application of metal frameworks.

In summary, firstly, the properties and preparation process of MOF (UIO-66)/ZrAl ceramic composite membranes are comprehensively discussed. Then, the theoretical knowledge of multisensor technology fused with machine learning is outlined. Finally, a multisensor model incorporating machine learning is designed based on the controllable fabrication concept of MOF (UIO-66)/ZrAl ceramic composite membranes. The innovation lies in breaking through the traditional preparation method of the MOF (UIO-66)/ZrAl ceramic composite membrane and creating a novel controllable preparation technology. The research not only provides technical support for the development of multisensor technology incorporating machine learning but also contributes to the controllable preparation of composite membranes.

## 2. Methods

*2.1. The Basic Idea of Metal-Organic Frameworks.* MOFs and supramolecular coordination complexes (SCCs) are collectively referred to as metal-organic materials (MOMs). MOFs refer to metal ions or metal clusters and organic ligands matching each other through their own bonds to form a one-dimensional or multidimensional infinite network structure. This material has a new type of crystalline complex with three-dimensional pores and has the characteristics of strong ligand-metal interaction, crystallinity, and porosity [6]. MOFs were proposed in 1995 and had many advantages. The more prominent ones are large porosity and surface area, and their powerful functions also have the advantages of size controllability and so on. Therefore, when using MOF materials, their structures can be designed and modified according to the requirements to realize the modification and regulation of their functions, and a new generation of membrane materials can be obtained. However, the preparation of MOF films with better compactness and functional regulation and modification is still less. Due to the size difference between the MOF film and gas molecules and the molecular weight difference between gas molecules, in most cases, it is very difficult to separate gas molecules with similar molecular weight and size well. Therefore, it has become a new method to utilize the interaction between gas molecules and functional groups on the surface of MOF membrane pores to achieve efficient gas separation. This method has also been favored by many researchers [7].

In applying metal framework films, the storage and classification of small molecules is a widely used purpose, such as the storage of  $H_2$ ,  $CO_2$ , and  $CH_4$ . In 2003, the phenomenon that metal framework compounds were used to store  $H_2$  was reported, and about 200 kinds of metal framework compounds can store  $H_2$ . In terms of natural gas storage, the separation of  $H_2$  from  $CH_4$  is an important process. In the separation process, the impact of  $CO_2$  should be reduced. It includes the blockage of  $CO_2$  on natural gas pipelines and the impact on the natural environment. Therefore, the use of metal framework materials for  $CO_2$  separation has become a current research hotspot [8].

At present, many groups have successfully fabricated metal framework films and have also proposed many fabrication methods to point out the application value of metal framework films. The preparation of the metal skeleton film mainly depends on the secondary growth process of the metal skeleton powder. The film can be directly prepared from the metal skeleton powder, and the film preparation requirements can be met through its growth. However, the degree of controllability is too low, and the preparation results are not ideal. The current relatively advanced preparation method uses functional group-modified metal as a carrier to prepare membranes. A typical example is the preparation process for MOF-5. The main principle is to make the crystal and the carrier tightly combined to form an ideal membrane structure. The main principle of its utilization is the secondary growth method of metal skeleton powder. However, this method improves the controllability of the membrane, and its practicality is relatively high [9]. The basic structure of MOF is shown in Figure 1.

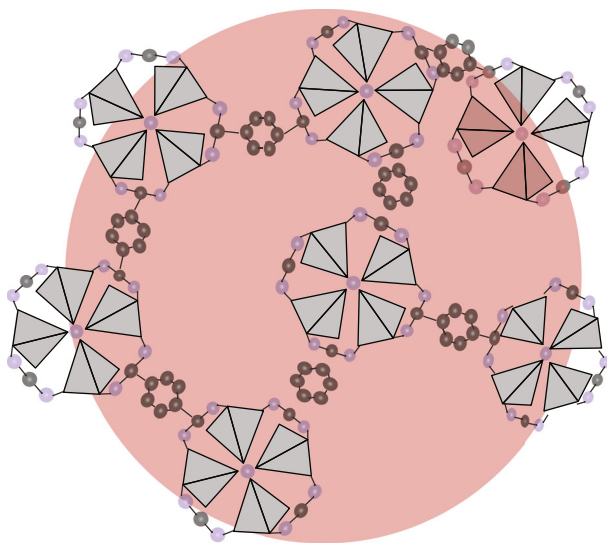


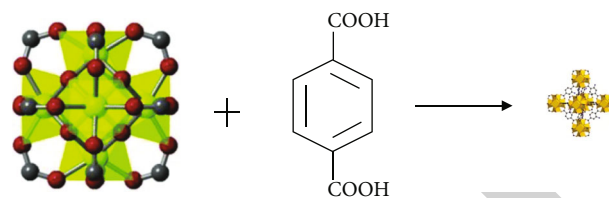
FIGURE 1: Basic structure of MOF.

In Figure 1, the preparation process of MOF films is not only stable but also highly efficient. On metal supports, different concepts are derived from growing metal frameworks to prepare films. First, it is directly grown or deposited in the mother liquor, that is, prepared by deposition in the liquid made of MOF powder. Next, the crystals are individually synthesized and then assembled into films. Then, the MOFs are grown on the support layer by layer to form a film, or the MOFs are electrochemically deposited on the metal support to form a film, that is, a method of growing another MOF film on the MOF film. Finally, the sandwich method deposited MOF films [10].

**2.2. UIO-66 Series.** UIO-66 is a three-dimensional porous framework formed by the metal ion structural unit  $Zr_6O_4(OH)_4$  connected with 12 organic ligands, respectively. UIO-66 has super stability. This feature mainly relies on the matching Zr-O bond between terephthalic acid ( $H_2BDC$ ) and the structural unit  $Zr_6O_4(OH)_4$ , which also explains its wide application in sewage treatment and heterogeneous catalysis [11]. The schematic diagram of the complex structure of UIO-66 and the structural unit  $Zr_6O_4(OH)_4$  stimulation unit and their synthesis is shown in Figure 2.

In Figure 2,  $Zr_6O_4(OH)_4$  is an octahedral structure unit. There are six  $Zr^{4+}$  ions in its octahedral structure unit and four oxygen atoms or hydroxyl groups at each small interface center point of its eight interfaces [12]. These metal nodes are individually coordinated to twelve  $H_2BDC$  ligands, thereby coordinating Zr atoms to eight oxygen atoms in  $H_2BDC$ . Finally, the theoretical pore volume and theoretical surface area of UIO-66 are  $0.45\text{ cm}^3/\text{g}$  and  $1018\text{ m}^2/\text{g}$ , respectively. The actual surface area of UIO-66 is usually between  $800$  and  $1200\text{ m}^2/\text{g}$ , depending on its preparation method [13]. The main structures of UIO-66 and its secondary components are shown in Figure 3.

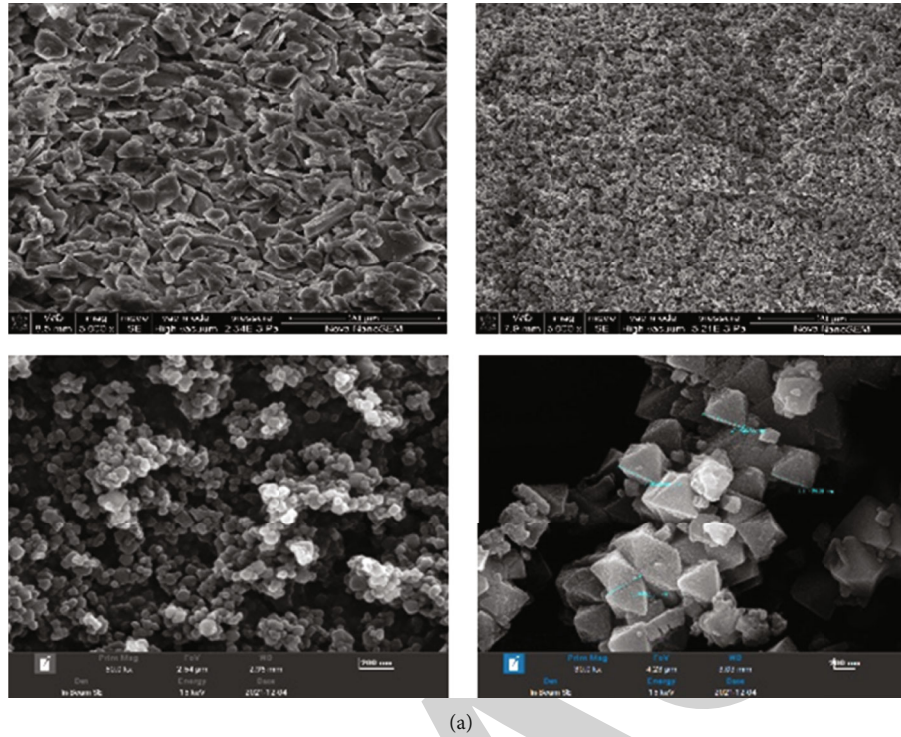
Figure 3 shows the spatial structures of  $Al_2O_3$  and UIO-66 at different scales and the structure of their fusion product  $Al_2O_3-ZrO_2$ . Different structures of UIO-66 have differ-

FIGURE 2: Schematic representation of the complex structure of UIO-66 and the building block  $Zr_6O_4(OH)_4$  stimulation unit and their synthesis.

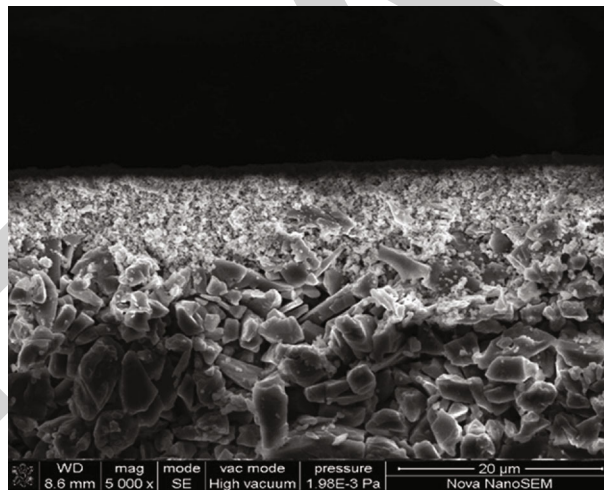
ent functions. Therefore, controllable preparation of UIO-66 according to its different functions and properties of different spatial structures is a method to utilize UIO-66 complexes [14] effectively. UIO-66 is generally prepared by accurately weighing  $0.053\text{ g}$  of  $ZrCl_4$  ( $0.227\text{ mmol}$ ) into  $24.9\text{ g}$  of DMF ( $340\text{ mmol}$ ) solvent and sonicated to dissolve completely. Then,  $0.034\text{ g}$  of  $C_8H_6O_4$  ( $0.227\text{ mmol}$ ) is added to the solvent, dissolved by ultrasonic vibration, and uniformly mixed. Then, the mixed solution is transferred into a  $50\text{ ml}$  autoclave. The reaction kettle is placed in an oven and reacted at  $120^\circ\text{C}$  for  $24\text{ h}$ . After the reaction, it is naturally cooled to room temperature, and the reaction kettle is taken out and filtered with suction. Then, chloroform and methanol are alternately washed for one day. Finally, the reagent is filtered and vacuum dried, and the white product UIO-66 is obtained [15]. The structure of the UIO-66 complex is relatively subtle, and it is difficult to control it during the preparation process. Therefore, this problem has become the main research project for the preparation of UIO-66 at present.

**2.3. Multisensor Controllable Technology Incorporating Machine Learning.** Today, with the development of science and technology, sensors have developed rapidly, providing a lot of convenience for the development of human beings. With the expansion of its application range, more and more types of performance have also been greatly improved. Therefore, this greatly promotes the generation of multisensor systems for different application backgrounds. In complex multisensor systems, the diversity of data types, huge data capacity, and the relationship between complex data and information will lead to the traditional data fusion methods that can no longer meet the requirements of complex systems [16] for high-precision and high-speed data fusion. Therefore, how to accurately and quickly fuse multidimensional data from different information systems and multiple sensors, quickly carry out more accurate, efficient, and reasonable fusion, and make an accurate estimation has become an urgent problem to be solved. This multisensor system needs to use new methods to process many multidimensional data. In this application background, a new data processing method, that is, the multisensor data fusion technology method, came into being [17].

As a new science and technology type, machine learning has become a current innovative technology by integrating with sensors. Machine learning is a multidomain interdisciplinary subject involving probability theory, statistics, approximation theory, convex analysis, algorithm complexity theory,



(a)



(b)

FIGURE 3: The main structures of UIO-66 and its secondary components are (a) the two structures of  $\text{Al}_2\text{O}_3$  and UIO-66 and (b) the structure of  $\text{Al}_2\text{O}_3\text{-ZrO}_2$ .

and other disciplines. It specializes in how computers simulate or realize human learning behaviors to acquire new knowledge or skills and reorganize existing knowledge structures to improve their performance continuously. It is the core of artificial intelligence and the fundamental way to make computers intelligent [18]. Machine learning encompasses a variety of techniques. Among them, Backpropagation Neural Network (BPNN) technology, as an advanced machine learning technology, can provide important technical support for the fusion of various sensors. When BPNN is applied to multisensor data fusion, it is necessary to select an appropriate neural network model. The selection criteria are the requirements of the fusion system and the characteristics of the sensors, including net-

work topology, neuron characteristics, and learning rules [19]. Additionally, the connection between input and sensor information, output, and system decision-making is established. Then, the distribution of weights is determined according to the acquired sensor information and the corresponding system decision-making information to complete the training of the network [20]. BPNN has arbitrarily complex pattern classification ability and excellent multidimensional function mapping ability and solves some problems that simple perceptrons cannot solve. Structurally, BPNN has an input layer, a hidden layer, and an output layer. In essence, BPNN takes the square of the network error as the objective function and uses the gradient descent method to calculate the minimum

value of the objective function. The basic BPNN includes two processes signal forward propagation and error backpropagation [21]. Error outputs are calculated in the input-to-output direction, and weights and thresholds are adjusted in the output-to-input direction. During forward propagation, the input signal acts on the output node through the hidden layer, and after nonlinear transformation, the output signal is generated. If the actual output does not match the expected output, it turns to the backpropagation process of the error [22]. Error backpropagation is to backpropagate the output error layer by layer to the input layer through the hidden layer, distribute the error to all units in each layer, and use the error signal obtained from each layer as the basis for adjusting the weights of each unit. By adjusting the connection strength between the input node and the hidden layer node, the connection strength between the hidden layer node and the output node, and the threshold, the error decreases along the gradient direction. After repeated learning and training, the network parameters (weights and thresholds) corresponding to the minimum error are determined. At this time, the trained neural network can automatically process the nonlinearly transformed information with the smallest output error for the input information of similar samples [23]. The principle of neural network technology fusion multisensor technology is shown in Figure 4.

In Figure 4, BPNN technology provides important support for the development of sensor technology. Radial basis function (RBF) neural network models optimize multisensor fusion techniques. Therefore, the designed model is RS-BP (radial sensor backpropagation) multisensor data fusion technology [24]. Among them, RBF neural network technology is the main technology of this model. Its activation function is shown in

$$R(\|\text{dist}\|) = e^{-\|\text{dist}\|^2}. \quad (1)$$

$\|\text{dist}\|$  represents the distance between the input vector and the weight. There are four radial basis functions of the RBF neural network model, which are thin-plate spline function, multiquadratic function, inverse multiquadratic function, and Gaussian function, as shown in

$$\phi(x) = x^2 \lg(x), \quad (2)$$

$$\phi(x) = (x^2 + c)^{1/2}, \quad c > 0, \quad (3)$$

$$y_k = \sum_{j=1}^j w_{jk} h_j(x), \quad k = 1, 2, \dots, K, \quad (4)$$

$$\phi(x) = \exp\left(-\frac{x - c_j}{2\sigma_j^2}\right). \quad (5)$$

$x$  represents the input vector,  $c$  and  $k$  represent the fixed parameters,  $w$  represents the weight,  $j$  represents the input vector sequence, and  $\sigma$  represents the variance of the Gaussian function [25]. The RBF neural network has input, output, and hidden layers. Among them, the node calculation

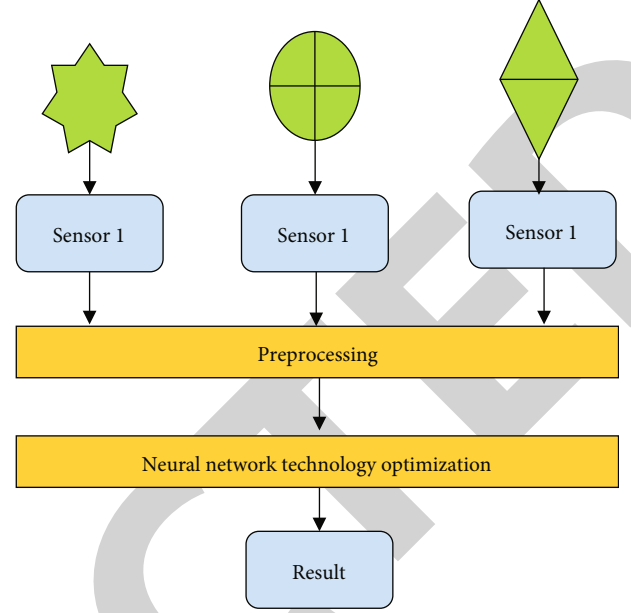


FIGURE 4: The principle of neural network technology fusion multisensor technology.

of the hidden layer is shown in

$$n = \sqrt{m + p} + d. \quad (6)$$

$n$  represents the number of nodes in the hidden layer,  $m$  represents the number of nodes in the input layer,  $p$  represents the number of nodes in the output layer, and  $d$  is a fixed constant. The calculation of the output layer result is shown in

$$h_j(x) = \phi\left(-\frac{X - c_j}{\sigma_j}\right), \quad j = 1, 2, \dots, J. \quad (7)$$

$j$  represents the position of the calculation element in the output layer,  $\sigma_j$  represents the center of the Gaussian function,  $c_j$  represents the variance of the Gaussian function, and the remaining parameters are the same as the above equations [26]. However, the model still needs to be trained. Therefore, the training results are calculated as

$$E = \frac{1}{2} e^2, \quad (8)$$

$$\Delta c_j = \eta \frac{w_j}{\delta_j^2} e \sum_{i=1}^M G(X_i - c_j) (X_i - c_j), \quad (9)$$

$$\Delta \delta_j = \eta \frac{w_j}{\delta_j^3} e \sum_{i=1}^M G(X_i - c_j) (X_i - c_j)^2, \quad (10)$$

$$\Delta w_j = \eta e \sum_{i=1}^M G(X_i - c_j). \quad (11)$$

$G$  is a Gaussian function, and  $c_j$ ,  $\delta_j$ , and  $w_j$ , respectively, represent the weights between the three levels of the RBF

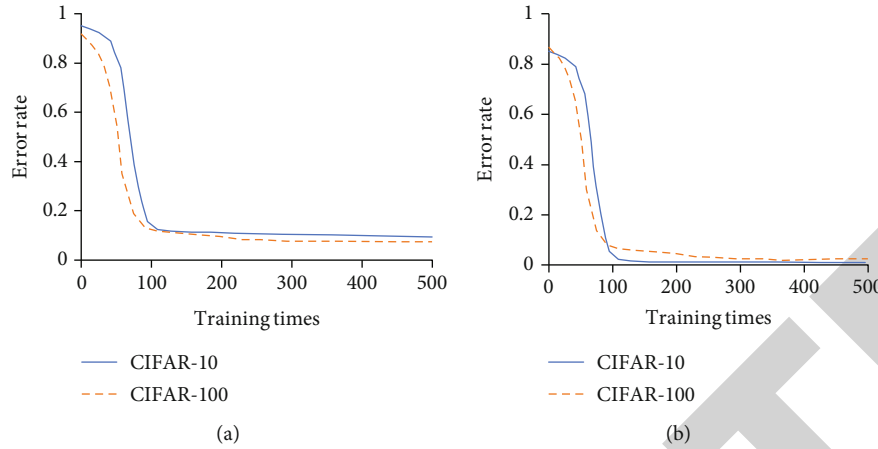


FIGURE 5: The training results of (a) the RBF neural network model and (b) the RS-BP multifusion sensor model.

neural network [27]. The activation function of the RBF neural network is shown in

$$R(x_p - c_i) = \exp\left(-\frac{1}{2\sigma^2}x_p - c_i^2\right). \quad (12)$$

$x_p - c_i$  represents the Euclidean norm and  $c_j$  represents the center of the Gaussian function [28]. The output of the network structure is shown in

$$y_j = \sum_{i=1}^h w_{ij} \exp\left(-\frac{1}{2\sigma^2}x_p - c_i^2\right). \quad (13)$$

The variance calculation of the Gaussian function is shown in

$$\sigma = \frac{1}{P} \sum_j^m d_j - y_j c_i^2. \quad (14)$$

$d$  represents the network sample data [29]. Firstly, the designed RS-BP model is trained, and the model's performance is evaluated. The datasets selected for training are Canadian Institute for Advanced Research-10 (CIFAR-10) and CIFAR-100 datasets, respectively. Among them, the CIFAR-10 dataset contains a total of 60,000 colors (RGB) images with a size of  $32 * 32$ . Among the 60,000 images, 50,000 are used as training sets and 10,000 are used for testing. There are 100 categories in the CIFAR-100 dataset, and each category has 600 images. The CIFAR-100 dataset contains many samples, which provides a sufficient basis for model evaluation. Among them, the sample conforms to the design connotation of the model. Therefore, it is very reasonable that the CIFAR-100 dataset is chosen as the training dataset. Then, MOF (UIO-66) ZrAl ceramic composite films are prepared by using a model and sensor, and corresponding tests evaluate the products.

### 3. Results

**3.1. Evaluation of Multisensor Technologies Incorporating Machine Learning.** The fusion machine learning multisensor technology can not only fuse the performance of multiple sensors but also optimize the performance of the fusion sensor through RBF neural network technology so as to design a fusion sensor device that can comprehensively identify and provide accurate data. This can provide technical support for the controllable preparation of MOF (UIO-66) ZrAl ceramic composite films. The training results of the RBF neural network model and the RS-BP fusion multisensor model are shown in Figure 5.

In Figure 5, in the training results of the RBF neural network model, the highest error rate of the model is around 0.90, and the overall error rate of the training results in the two datasets decreases rapidly. When the number of training times reaches 100, the model's error rate is basically stable, and the minimum error rate is about 0.09. In the training results of the RS-BP multifusion sensor model, the error rate of the training results of the two datasets is the highest at about 0.87. When the training is about 100 times at this time, the model's error rate tends to be stable, and the error rate is the lowest at about 0.01.

**3.2. Controllable Preparation of MOF (UIO-66) ZrAl Ceramic Composite Membranes.** The preparation process of the MOF (UIO-66) ZrAl ceramic composite membrane is complicated, and its structure is difficult to control artificially. Therefore, contemporary science and technology is innovative research on its controllable preparation. The preparation of MOF (UIO-66) ZrAl ceramic composite membranes is studied by the multisensor model technology fused with machine learning. Figure 6 shows the comparison of the performance of the films made by traditional preparation and fusion multisensor preparation methods.

In Figure 6, under the traditional preparation method, a relatively fixed composite membrane preparation method is formulated through the support of theoretical knowledge. This study has a relatively weak ability to control the preparation process, and the membrane performance is relatively

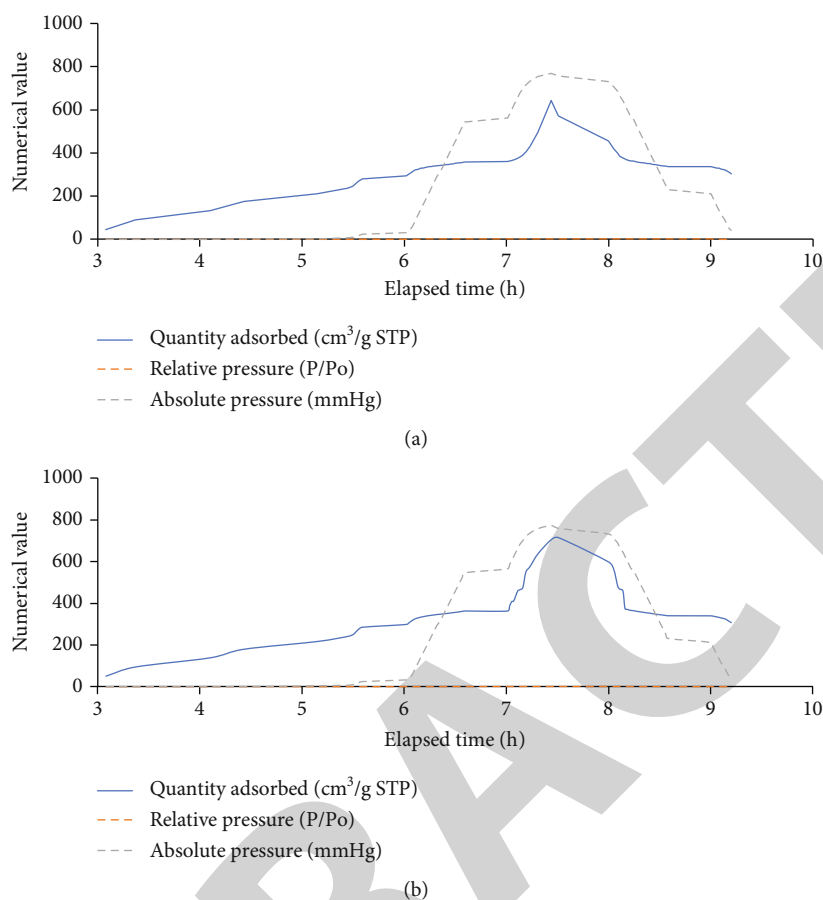


FIGURE 6: Comparison of the performance of films made by (a) traditional preparation and (b) fusion multisensor preparation.

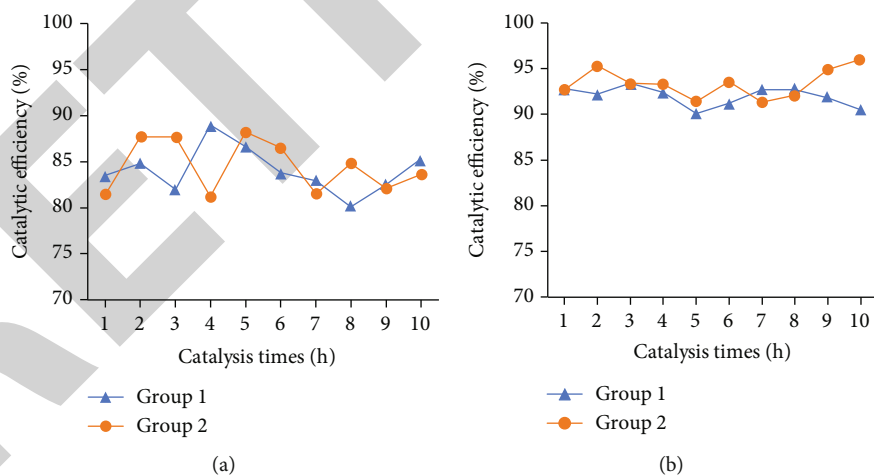


FIGURE 7: Evaluation of the catalytic performance of UIO-66 composite membrane: (a) the traditional preparation method and (b) the preparation method of fusion of multiple sensors.

weak. The gas adsorption capacity of the traditional film preparation method increased significantly at about 7 hours, and the maximum is 700 cm<sup>3</sup>/g STP, and it decreased rapidly after reaching the highest adsorption capacity. Therefore, the overall adsorption capacity is relatively low. The preparation method of the fusion multisensor can control the properties of the membrane according to the properties of the prepara-

tion components and the comprehensive changes in the reactor during the preparation process and improve the adsorption capacity of the membrane. Therefore, the adsorption capacity of the fusion multisensor preparation method increased significantly in about 7 hours, and the maximum adsorption capacity is around 800 cm<sup>3</sup>/g STP. Additionally, the adsorption capacity decreased slowly, and



the overall adsorption energy is higher than that of the traditional preparation method. In order to reflect the advantages of the designed model, the designed model is compared with the traditional preparation method through two groups of studies, which improves the value of the comprehensive performance evaluation of the model. Figure 7 shows the photocatalytic performance evaluation of UiO-66 composite films under different preparation methods.

In Figure 7, under the traditional preparation method, the catalytic efficiency of the membrane is about 80%-88%. The vegetation method that fuses multiple sensors can control the microstructure of the membrane to prepare a membrane with strong comprehensive performance. Therefore, the catalytic efficiency of membranes prepared by fusing multiple sensors is around 90%-97%.

#### 4. Conclusion

This study is aimed at improving the comprehensive properties of MOF (UiO-66)/ZrAl ceramic composite membranes and improving the utilization efficiency of various resources. Firstly, the preparation process and properties of MOF (UiO-66)/ZrAl ceramic composite membranes are discussed. Then, the technical concept of machine learning fusion of multisensors is outlined. Finally, the controllable preparation technology of the MOF (UiO-66)/ZrAl ceramic composite membrane is designed by fusing neural network technology and multisensor. The results show that the error rate of the designed RS-BP fusion multisensor model training results is about 0.87. When the number of training is about 100 times, the model's error rate tends to be stable, and the minimum error rate is about 0.01. Secondly, the maximum adsorption capacity of the composite membrane under the controllable preparation of the model is about 800 cm<sup>3</sup>/g STP, and the adsorption capacity decreases slowly. Therefore, the overall adsorption energy is higher than that of the traditional preparation method. Finally, the catalytic efficiency of the membrane prepared by fusing multiple sensors is 90%-97%, which significantly improves the comprehensive performance of the composite membrane. Although this study has designed a relatively complete RS-BP multifusion sensor model, the research on its comprehensive application in practice is not perfect. Therefore, in the future, the research in this field and the development and comprehensive application of sensor fusion machine learning technology will be further strengthened.

#### Data Availability

The data used to support the findings of this study are included within the article.

#### Conflicts of Interest

The authors declare that they have no conflicts of interest.

#### Acknowledgments

This work was sponsored in part by the Natural Science Research Project of Anhui Department of Education (KJ2021A1021), Natural Science Foundation of Anhui Province (1908085ME153), and Chaohu University scientific research project (XLY-201916).

#### References

- [1] J. Fonseca, T. Gong, L. Jiao, and H. L. Jiang, "Metal-organic frameworks (MOFs) beyond crystallinity: amorphous MOFs, MOF liquids and MOF glasses," *Journal of Materials Chemistry A*, vol. 9, no. 17, pp. 10562–10611, 2021.
- [2] N. Shaukat, A. Ali, M. Javed Iqbal, M. Moinuddin, and P. Otero, "Multi-sensor fusion for underwater vehicle localization by augmentation of RBF neural network and error-state Kalman filter," *Sensors*, vol. 21, no. 4, p. 1149, 2021.
- [3] N. Shaukat, A. Ali, M. Javed Iqbal, M. Moinuddin, and P. Otero, "Metal-organic frameworks (MOFs) based electrochemical biosensors for early cancer diagnosis in vitro," *Coordination Chemistry Reviews*, vol. 439, no. 3, article 213948, 2021.
- [4] S. Li, Y. Gao, N. Li, L. Ge, X. Bu, and P. Feng, "Transition metal-based bimetallic MOFs and MOF-derived catalysts for electrochemical oxygen evolution reaction," *Energy & Environmental Science*, vol. 14, no. 4, pp. 1897–1927, 2021.
- [5] V. Shepelev, S. Aliukov, K. Nikolskaya, A. Das, and I. Slobodin, "The use of multi-sensor video surveillance system to assess the capacity of the road network," *Transport and Telecommunication*, vol. 21, no. 1, pp. 15–31, 2020.
- [6] K. Wang, Q. Li, Z. Ren et al., "2D metal-organic frameworks (MOFs) for high-performance BatCap hybrid devices," *Small*, vol. 16, no. 30, article 2001987, 2020.
- [7] Y. Yan, C. Li, Y. Wu, J. Gao, and Q. Zhang, "From isolated Ti-oxo clusters to infinite Ti-oxo chains and sheets: recent advances in photoactive Ti-based MOFs," *Journal of Materials Chemistry A*, vol. 8, no. 31, pp. 15245–15270, 2020.
- [8] J. B. Pan, B. H. Wang, J. B. Wang et al., "Activity and stability boosting of an oxygen-vacancy-rich BiVO<sub>4</sub> photoanode by NiFe-MOFs thin layer for water oxidation," *Angewandte Chemie International Edition*, vol. 60, no. 3, pp. 1433–1440, 2021.
- [9] M. Wang, R. Dong, and X. Feng, "Two-dimensional conjugated metal-organic frameworks (2Dc-MOFs): chemistry and function for MOFtronics," *Chemical Society Reviews*, vol. 50, no. 4, pp. 2764–2793, 2021.
- [10] M. Lv, W. Zhou, H. Tavakoli et al., "Aptamer-functionalized metal-organic frameworks (MOFs) for biosensing," *Biosensors and Bioelectronics*, vol. 176, no. 8, article 112947, 2021.
- [11] X. Liu, "Metal-organic framework UiO-66 membranes," *Frontiers of Chemical Science and Engineering*, vol. 14, no. 2, pp. 216–232, 2020.
- [12] N. Rabiee, M. Bagherzadeh, M. Heidarian Haris et al., "Polymer-coated NH<sub>2</sub>-UiO-66 for the codelivery of DOX/pCRISPR," *ACS Applied Materials & Interfaces*, vol. 13, no. 9, pp. 10796–10811, 2021.
- [13] G. Wang, C. T. He, R. Huang, J. Mao, D. Wang, and Y. Li, "Photoinduction of Cu single atoms decorated on UiO-66-NH<sub>2</sub> for enhanced photocatalytic reduction of CO<sub>2</sub> to liquid fuels," *Journal of the American Chemical Society*, vol. 142, no. 45, pp. 19339–19345, 2020.

- [14] M. Li, Y. Liu, F. Li et al., "Defect-rich hierarchical porous UiO-66(Zr) for tunable phosphate removal," *Environmental Science & Technology*, vol. 55, no. 19, pp. 13209–13218, 2021.
- [15] B. Zhao, L. Yuan, Y. Wang, T. Duan, and W. Shi, "Carboxylated UiO-66 tailored for U(VI) and Eu(III) trapping: from batch adsorption to dynamic column separation," *ACS Applied Materials & Interfaces*, vol. 13, no. 14, pp. 16300–16308, 2021.
- [16] L. Wu, L. Chen, and X. Hao, "Multi-sensor data fusion algorithm for indoor fire early warning based on BP neural network," *Information*, vol. 12, no. 2, p. 59, 2021.
- [17] S. Teng, G. Chen, Z. Liu, L. Cheng, and X. Sun, "Multi-sensor and decision-level fusion-based structural damage detection using a one-dimensional convolutional neural network," *Sensors*, vol. 21, no. 12, p. 3950, 2021.
- [18] J. J. Zhang, Z. Y. Ye, and Z. Y. Li, "Multi-sensor information fusion detection system for fire robot through back propagation neural network," *Plos one*, vol. 15, no. 7, article e0236482, 2020.
- [19] J. Hu, B. Zheng, C. Wang et al., "A survey on multi-sensor fusion based obstacle detection for intelligent ground vehicles in off-road environments," *Frontiers of Information Technology & Electronic Engineering*, vol. 21, no. 5, pp. 675–692, 2020.
- [20] J. Lv, C. Qu, S. Du et al., "Research on obstacle avoidance algorithm for unmanned ground vehicle based on multi-sensor information fusion," *Mathematical Biosciences and Engineering*, vol. 18, no. 2, pp. 1022–1039, 2021.
- [21] W. Qi, S. E. Ovrur, Z. Li, A. Marzullo, and R. Song, "Multi-sensor guided hand gesture recognition for a teleoperated robot using a recurrent neural network," *IEEE Robotics and Automation Letters*, vol. 6, no. 3, pp. 6039–6045, 2021.
- [22] M. Wang, K. Tan, X. Jia, X. Wang, and Y. Chen, "A deep Siamese network with hybrid convolutional feature extraction module for change detection based on multi-sensor remote sensing images," *Remote Sensing*, vol. 12, no. 2, p. 205, 2020.
- [23] S. Han, J. Xu, M. Yan, and Z. Liu, "Using multiple linear regression and BP neural network to predict critical meteorological conditions of expressway bridge pavement icing," *Plos one*, vol. 17, no. 2, article e0263539, 2022.
- [24] C. Liu, Y. Feng, and Y. Wang, "An innovative evaluation method for undergraduate education: an approach based on BP neural network and stress testing," *Studies in Higher Education*, vol. 47, no. 1, pp. 212–228, 2022.
- [25] Y. Deng, X. Zhou, J. Shen et al., "New methods based on back propagation (BP) and radial basis function (RBF) artificial neural networks (ANNs) for predicting the occurrence of halo-ketones in tap water," *Science of The Total Environment*, vol. 772, no. 2, article 145534, 2021.
- [26] Q. Li, Q. Xiong, S. Ji, Y. Yu, C. Wu, and H. Yi, "A method for mixed data classification base on RBF-ELM network," *Neurocomputing*, vol. 431, no. 3, pp. 7–22, 2021.
- [27] Y. Zhou, X. Zhang, and F. Ding, "Hierarchical estimation approach for RBF-AR models with regression weights based on the increasing data length," *IEEE Transactions on Circuits and Systems II: Express Briefs*, vol. 68, no. 12, pp. 3597–3601, 2021.
- [28] X. Zhang, P. Zhang, T. Wang, Y. Zheng, L. Qiu, and S. Sun, "Compressive strength and anti-chloride ion penetration assessment of geopolymer mortar merging PVA fiber and nano-SiO<sub>2</sub> using RBF-BP composite neural network," *Nanotechnology Reviews*, vol. 11, no. 1, pp. 1181–1192, 2022.
- [29] L. Bai, K. Zheng, Z. Wang, and J. Liu, "Service provider portfolio selection for project management using a BP neural network," *Annals of Operations Research*, vol. 308, no. 1-2, pp. 41–62, 2022.